Viscoelastic Fracture of Solid Propellants in Pressurization Loading Conditions

E. C. FRANCIS* AND C. H. CARLTON†
United Technology Center, Sunnyvale, Calif.
AND
G. H. LINDSEY‡
Naval Postgraduate School, Monterey, Calif.

An analytical technique is presented for predicting structural failures of flawed solid propellant rocket motors during ignition. The technique uses viscoelastic fracture mechanics as part of an engineering analysis. Viscoelastic fracture toughness behavior of a solid propellant and a nonfilled polymer were characterized with constant load and constant strain cracked biaxial sheet tests. Crack propagation rates were measured as a function of stress intensity factor and superimposed pressure. The fracture characteristics of solid propellant were significantly improved by the hydrostatic pressure generated by rocket motor ignition, while an unfilled polymer showed no pressure effect. Predicted rocket motor crack propagation behavior is compared in plane stress pressurized rocket models with propellant and an unfilled polymer. Measured crack velocity data from model tests with a linear viscoelastic material (Solithane 113) were in agreement with theoretical predictions. However, crack propagation could not be induced in solid propellant grain models because of the increase in fracture toughness in a hydrostatic stress field.

Nomenclature

a_T = temperature shift factor
$A(t)$ = time-dependent area
b = strip half-height; grain o.d.
B = pressure multiplicative factor
b/a = outside to inside (ratio)
c = crack length
$\dot{c}$ = crack velocity
c_o = initial crack length
$c(t)$ = time-dependent crack
E = Young's modulus
E_c = case modulus
E_{REL} = viscoelastic modulus
F = force
$f(\ )$ = function of
$g(\ )$ = function of
h = case thickness
K_I = stress intensity factor
$K_I^{(1)}$ = K_I without side pressure
$K_I^{(2)}$ = K_I with side pressure
K_{Ic} = fracture toughness
$K_{Is}^{v}(t)$ = viscoelastic stress intensity factor for a stationary crack
$K_I^{v}(t)$ = stress intensity factor for moving crack in viscoelastic material
L = sheet width
PBAN = polybutadiene-acrylic acid-acrylonitrile
r = radius
s = Laplace transform variable
t = time
Δ = increment
θ = polar coordinate
ν = Poisson's ratio
σ = stress
$\sigma(t)$ = time-dependent stress

Superscript
* = Laplace transform of

Presented as Paper 74-30 at the AIAA 12th Aerospace Sciences Meeting, Washington, D.C., January 30–February 1, 1974; submitted February 6, 1974; revision received April 19, 1974.

Index categories: Structural Static Analysis; Materials, Properties of; LV/M Structural Design (Including Loads).

* Supervisor, Propellant Evaluation, Propellant Development Branch.

† Head, Mechanical Properties Research, Propellant Development Branch. Member AIAA.

‡ Associate Professor, Department of Aeronautics.

Introduction

ROCKET grain fracture analyses have employed the energy balance theory of fracture mechanics for linearly viscoelastic materials. The energy balance criterion developed by Griffith[1] was extended to linear viscoelastic materials by Williams.[2] Williams[3] further showed that energy balance fracture criteria complement conventional failure criteria. Rocket grain fracture analysis generally requires determining stress intensity factors for complex geometries which are strongly influenced by boundary and loading conditions. Fracture initiation occurs only when the stress intensity factor for the specific geometry and loading condition is equal to, or greater than, the critical value for the material. For conditions which exceed the critical K_{Ic} value, crack velocities are a function of the material properties and the excess energy available to drive the crack.

The numerical analysis techniques currently used for rocket motor stress analysis are finite element computer formulations. Applications of these numerical techniques to evaluate stress intensity factors for different grain geometries are discussed in papers by Swanson,[4] Chan et al.,[5] and Kobayashi et al.[6] While stress intensity factors are obtainable to a reasonable accuracy by numerical techniques, the computer costs rise significantly with increased accuracy. However, Deverall and Lindsey[7] have demonstrated that stress intensity factors to $\pm 2\%$ can be obtained with modest grids. The fracture characterization methods developed analytically by Mueller[8] provided a crack displacement stress intensity factor relationship for a cracked sheet. Mueller and Knauss[9] applied this work to fracture characterization of a linear viscoelastic material. The basic elements of a viscoelastic fracture analysis, applicable to solid propellant grain designs, were presented by Knauss.[10]

This paper extends available viscoelastic fracture mechanics methods to a useful engineering analysis of rocket motor ignition conditions for pressure-loaded rocket grains. Crack velocity histories are predicted for two-dimensional grain slices exposed to pressurization conditions, and comparisons are made between predictions and experimental data.

Theory

The fracture of viscoelastic materials has been studied by extension of the elastic theory. The stress state near a crack tip in a symmetrically loaded elastic body is given by the classic expression

$$\sigma_{ij}(r,\theta) = K_I(E,\nu,\sigma,c)[2\pi r]^{-1/2} f_{ij}(\theta) \quad (1)$$

For viscoelastic materials, the crack propagates under all loads above a given low threshold; however, the rate of propagation is quite slow. Since the crack is propagating, the correspondence principle cannot be used because the Laplace transform is not defined for all times during the propagation. As an approximation, the crack is assumed to be held stationary so that the correspondence principle can be applied. From Eq. (1)

$$\sigma_{ij}{}^{v*}(r,\theta,s) = K_I[E^*(s),\sigma^*(s),c][2\pi r]^{1/2} f_{ij}(\theta) \quad (2)$$

Inverting Eq. (2) gives the stress field around the tip of a stationary crack in a viscoelastic material

$$\sigma_{ij}{}^{v}(r,\theta,t) = K_I{}^{v}[E_{\mathrm{REL}}(t),\sigma(t),c][2\pi r]^{-1/2} f_{ij}\theta \quad (3)$$

When the restriction that the crack be stationary is removed by attaching the coordinates origin to the crack tip, the stress field for a slowly moving crack becomes

$$\sigma_{ij}{}^{v}[r(t),\theta(t),t] = K_I{}^{v}[E_{\mathrm{REL}}(t),\sigma(t),c(t)][2\pi r(t)]^{-1/2} f_{ij}[\theta(t)] \quad (4)$$

Comparing Eqs. (1) and (4)

$$K_I{}^{v}(t) = L^{-1}\{K_I{}^{v}[E^*,\sigma^*,c]\}_{c\to c(t)} \quad (5)$$

This stress intensity factor was related to the fracture process, and an energy balance was made at the crack tip by Knauss[10] similar to the work done by Irwin for elastic fracture.

Knauss showed that fracture of viscoelastic materials is centered around a relationship between stress intensity factor and crack velocity. The fracture postulate for such materials states that, when a given value of stress intensity factor exists, there is a unique value of crack velocity associated with it regardless of geometry or loading. Fracture characterization of materials then requires that crack propagation tests be run on laboratory specimens, where K_I is independent of geometry, in this case thin sheets (Fig. 1). The elastic stress intensity factor for biaxial sheets is

$$K_I = Ev_1/2[(1-\nu^2)b]^{1/2} \quad (6)$$

where $v_1 = 2v_0$ is the crosshead displacement of the moving boundary. In terms of stress, this simplifies to

$$K_I = \sigma[b(1-\nu^2)]^{1/2} \quad (7)$$

where σ is the far-field stress in the sheet. The viscoelastic stress intensity factor from Eq. (5) (for $\nu = \frac{1}{2}$) is

$$K_I{}^{v}(t) = (3b/4)^{1/2}\sigma(t) \quad (8)$$

For sheets subjected to constant load, $\sigma(t) = F_o/A(t)$, the stress intensity factor to a very close approximation is

$$K_I{}^{v}(t) = [F_o/A(t)](3b/4)^{1/2} \quad (9)$$

where $A(t)$ is the net cross-sectional area, $[L-c(t)] \times$ sheet thickness. This relationship was verified to be within 1% error for 1- by 6-in. sheets containing cracks up to 3 in. long.

Solithane Characterization

Crack propagation tests were run for five temperatures and for various values of $K_I{}^{v}(t)$ as computed from Eq. (9). A master curve of K_I vs $\dot{c}$ is generated where the data have been shifted similarly to relaxation modulus. From these data, crack behavior was predicted for a plane stress model of a rocket motor cross section.

Crack velocity data for Solithane 113 were obtained from cracked biaxial strip tests. A cracked propellant specimen being tested is shown in Fig. 2. Test data for Solithane 113 were obtained for a constant strain test mode. Samples were tested over a temperature range of 32°–138°F, and data are presented in Fig. 3. All data were shifted to form one composite master curve using the WLF equation[11] to account for viscoelastic

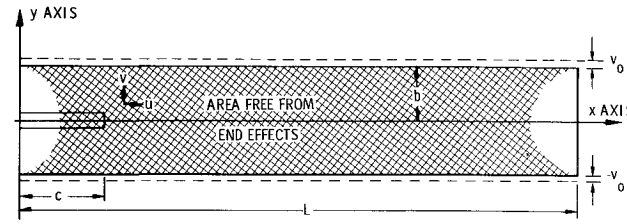

Fig. 1 Biaxial strip subjected to a uniform displacement, v_o.

effects. The modulus of Solithane 113 exhibited equilibrium behavior above 32°F, but the fracture behavior was temperature-dependent.

The curve drawn through the data in Fig. 3 represents the mean value of the K_I vs $\dot{c}$ response. The scatter of individual points is the accumulation of all experimental errors such as velocity measurements and modulus determinations that contribute to calculated K_I uncertainty for each test.

The selected crack velocity data range used for later model test comparisons is shown in Fig. 3 and was determined to provide reasonable experimental test times. For a given crack velocity in this range, the corresponding uncertainty in K_I is $\pm 16\%$. This is considered normal for fracture of viscoelastic materials.

Grain Predictions

Stress intensity factors were computed for different grain geometries as a function of the crack length. Numerical evaluation of K_I was conducted using a finite element computer code to determine strain energy release rates (dU/dA). These strain energy release rates were used with the plane stress equation of Irwin[12]

$$K_I{}^2 = E(dU/dA) \quad (10)$$

The finite element program used for the grain calculations was that developed by Rohm and Haas Co.[13] The mesh system used for one of the circular port grains (with a crack length of 1.00 in.) is shown in Fig. 4. The basic Rohm and Haas Co. computer program was modified to calculate the total energy in the grain. Strain energy release rates were determined from two successive computer calculations with a change in crack length of 0.050 in.

K_I was determined for two circular port designs ($b/a = 3.5$ and 4.5) and a six-pointed star design for different crack lengths

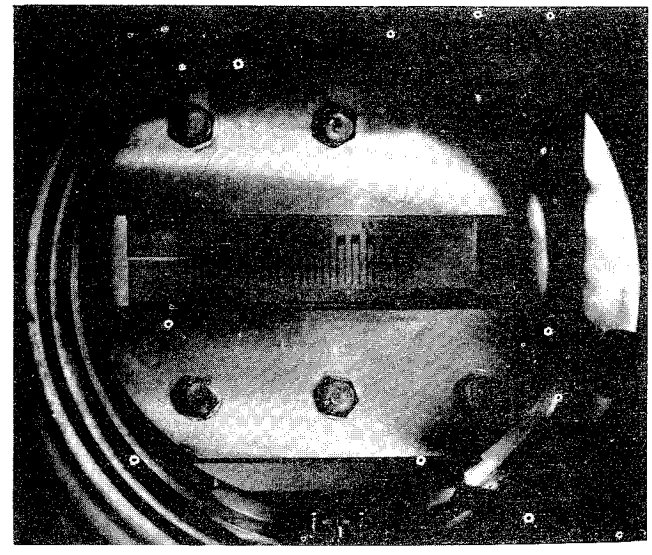

Fig. 2 Cracked biaxial propellant fracture specimen under test.

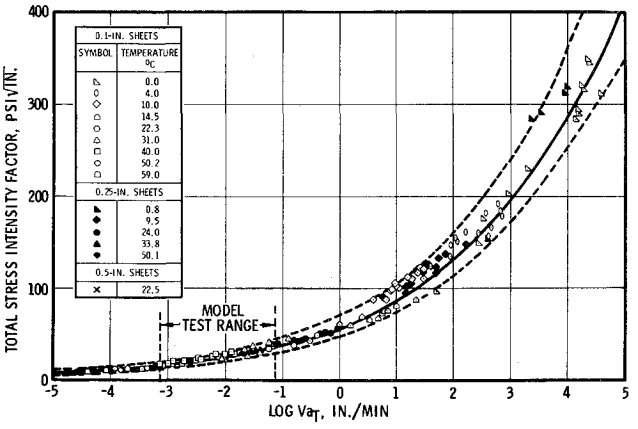

Fig. 3 Solithane 113 crack velocity vs stress intensity factor.

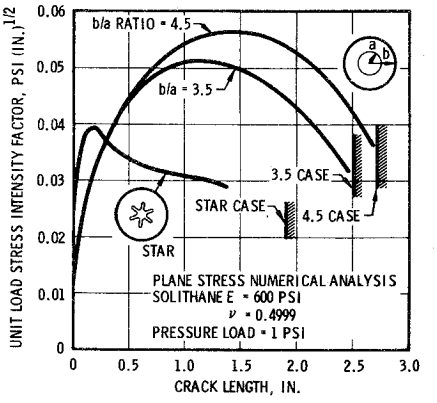

Fig. 5 Pressure K_I vs crack length for Solithane 113 star and circular port grains.

with Solithane 113. Results of the numerical analysis of the two-dimensional pressure tests for K_I are presented in Fig. 5. Both circular port grain K_I curves reach a maximum value when crack lengths extend about halfway through the grain. The star design K_I reaches a maximum value for a crack length of approximately 0.5 in. and then decreases slowly for increasing crack length. The rapid increase in K_I with crack length near the star tip is expected because the local field has a stress concentration in this region.

Effect of Face Pressure on Plane Stress Pressurization Analysis

Actual rocket motor grain pressurization conditions impose pressure internally and on the ends of the grain. The laboratory grain fracture pressurization equipment and experiments were designed to simulate actual rocket motor conditions so the two-dimensional stress analysis had to be modified to account for the face pressure. In the relationship between pressurization conditions with and without face pressure, $K_I^{(2)}$ with side pressure was related to the plane stress determined $K_I^{(1)}$ by Francis, Lindsey, and Parmerter[14] as

$$K_I^{(2)} = K_I^{(1)}/B \tag{11}$$

where B is a side pressure multiplicative factor which relates the two stress fields. This side pressure factor is evaluated from the following equation from Ref. 14:

$$B = \frac{(1-\nu)+(E/E_c)(b/h)}{(1-2\nu)+(E/E_c)(b/h)} \tag{12}$$

where E_c is the case modulus and h is the case thickness. The effect of the side pressure is to reduce the K_I determined from the plane stress numerical analysis.

With crack length vs K_I profiles for a grain design available, only the polymeric material fracture properties are required to define the crack velocity profile in the grain. The properties of the viscoelastic medium enter into the analysis in two ways. First, the local temperature influences the temperature shift factor (a_T). Second, a fundamental experimental determination of crack velocity vs stress intensity factor must be made. This is the crack velocity that results when the stress intensity factor is held constant, as in the case of the biaxial strip where the crack is large compared to the strip width.[9]

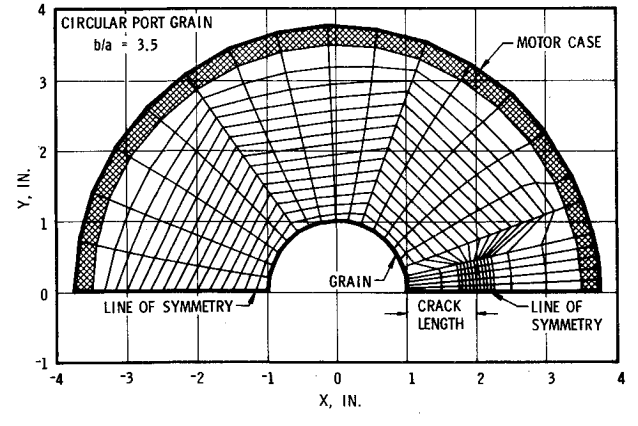

Fig. 4 Typical mesh for finite element computer analysis.

In developing the theory, several implicit assumptions have been made: 1) the distant stress field away from the crack tip is capable of description by an elastic solution, 2) the crack velocities are sufficiently low that dynamic or inertia effects are not induced in the grain, and 3) the relationship of the viscoelastic crack propagation equation to the elastic stress field can be described by a stress intensity factor (K_I).

The mathematical relationship used in the crack velocity analysis is as follows. First, the crack velocity is assumed to be related only to the stress intensity factor and to the temperature through the temperature shift factor (a_T). The crack velocity ($\dot{c}$) is related to the stress intensity factor (K_I) by[10]

$$dc/dt = \dot{c} = f(K_I, a_T) \tag{13}$$

If a crack in a grain has created some stress intensity factor, the same velocity will be experienced in any other configuration (e.g., a biaxial strip with that same stress intensity factor).

The essential experimental information to be added to Eq. (13) is the curve relating the value of K_I to $\dot{c}a_T$. This information is provided from a biaxial strip experiment with fixed grip displacement or constant load conditions. Experimentally derived K_I vs log ($\dot{c}a_T$) data are presented in Fig. 3.

As a result of Eq. (13), two equations for the stress intensity factor are $K_I = f(c)$ (from finite element grain analysis) and $K_I = g(\dot{c})$ (experimental relationship from strip tests).

For grain prediction, the theoretical K_I is set equal to the experimental K_I

$$g(\dot{c}) = f(c) \tag{14}$$

or

$$\dot{c} = g^{-1}f(c) = F(c) \tag{15}$$

This equation may be integrated to determine the crack length as a function of time. When the initial crack length (c_o) corresponds to time ($t = 0$), the initial crack velocity is equal to

$$\dot{c}_o = F(c_o) \tag{16}$$

For a small increase in time

$$\Delta c_o = F(c_o)\Delta t \tag{17}$$

$$c_1 = c_o + \Delta c_o \tag{18}$$

and the new crack velocity is

$$\dot{c}_1 = F(c_1) \tag{19}$$

$$\Delta c_1 = F(c_1)\Delta t \tag{20}$$

$$c_2 = c_1 + \Delta c_1 \tag{21}$$

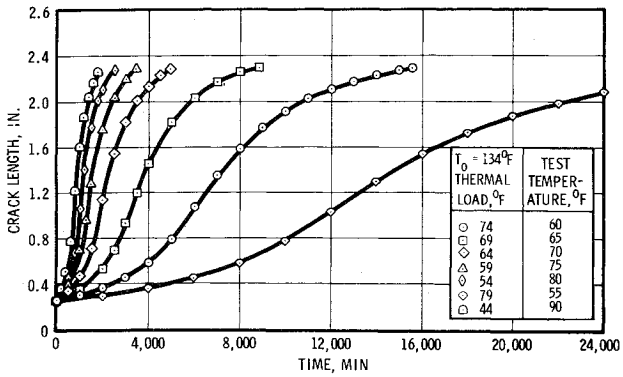

Fig. 6 Predicted crack tip motion for Solithane 113 fracture tests at 500 psi.

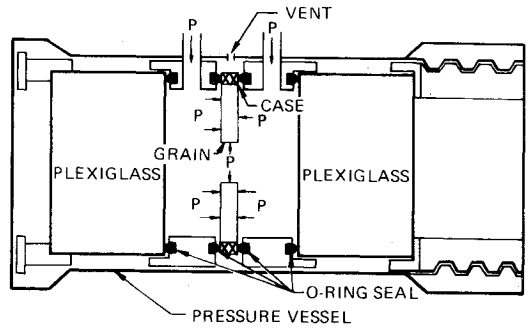

Fig. 8 Pressurization test equipment.

This iterative integration procedure was used to determine the crack length history. However, the time increments were small compared with the predictive time periods. For example, the selected time increments had to be 1 min or less with total crack travel times of 100 min to avoid integration errors. Predicted crack tip motion profiles for Solithane grain slices exposed to a test pressure of 500 psi at different temperatures are presented in Fig. 6.

Evaluation

The rocket model design selected for evaluating the theory consisted of a circular port grain with a b/a of 4.5 (Fig. 7). Solithane 113 grain slices were cast into Plexiglass rings to simulate a flexible rocket motor case. The zero stress temperatures, a function of the cure temperature and cure shrinkage for individual grains, were experimentally determined by thermal cycling until the bore diameter was equal to the mandrel dimension. Zero stress temperature for Solithane 113 was 134°F. After fracture testing, some zero stress temperatures were verified by thermal loading the grains until the crack just closed.

In preparation for pressure testing, a small crack (0.25–0.50 in.) was inserted at the inner perforation of each grain with a sharp razor blade. Pressure fracture tests were performed in a specially designed chamber for the two-dimensional grain slices (Fig. 8). O-ring seals on the sides of the plastic case permitted the case to deform radially under pressure. The chamber was rapidly filled with nitrogen to the desired pressure level and held constant during the test period. Crack growth was monitored through the plexiglass windows of the pressure vessel. Backlighting was used to enhance the crack tip definition. The data were recorded using motion pictures, as well as fast-framing still cameras.

The pressure test results are presented for the Solithane 113 grains in Fig. 9. The crack growth curves were started at 0.5 in. to eliminate erratic behavior shown during the "cut" to "natural" crack transition. Once the crack had established its own inherent crack tip geometry (approximately one sheet thickness), further crack growth was steady. This same crack startup behavior was noted in the biaxial sheet test specimens. Crack velocity increased as the crack length extended from the bore region to the central web region and then slowed down, approaching zero velocity as predicted. The pressure loads from 394 to 500 psig were selected to maintain reasonable experimental test times.

Propellant Fracture

Having demonstrated that this theory provides reasonable predictions of reality for unfilled materials, it was applied to plane stress rocket motor cross sections fabricated from propellant and subjected to pressure loads. The composite nature of the material raises the question of the influence of pressure on the fracture behavior; consequently, sheet tests for propellant were run in a pressurized environment. Because the material is incompressible, the pressure does not produce dilatational strain energy, and Irwin's relationship between strain energy change and stress intensity factor is unaffected by the addition of pressure. Therefore, the elastic stress intensity factor remains as given in Eq. (7), and the associated viscoelastic stress intensity factor is given in Eq. (9).

Although the stress intensity factor is unaffected by the pressure, the physical behavior of the material is influenced by it. Solid propellant tests were performed using a constant load test

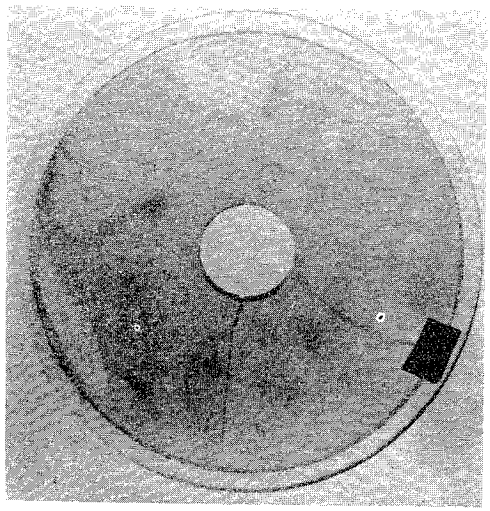

Fig. 7 Solithane grain after pressure testing.

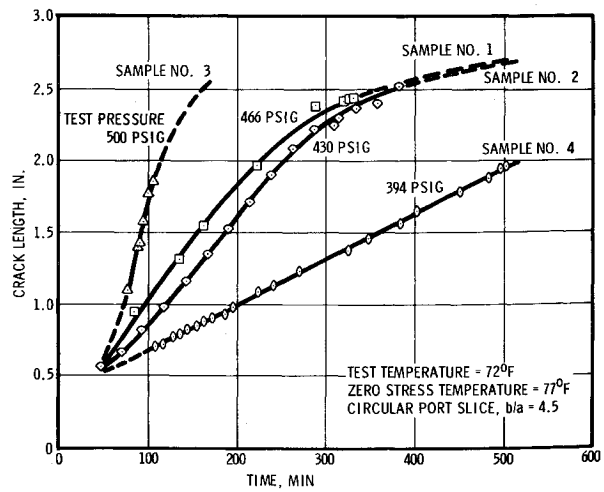

Fig. 9 Pressurized crack displacement measurements for Solithane grains.

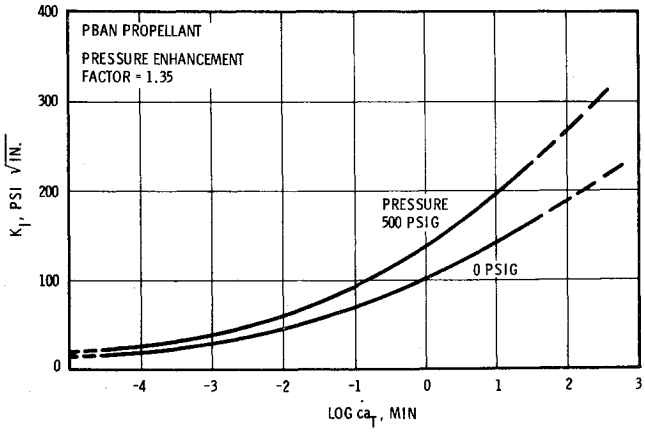

Fig. 10 Master K_I vs crack velocity curves for PBAN propellant.

mode because modulus relaxation occurred very rapidly, making it impossible to obtain reliable constant strain data. The constant load mode yielded a nearly constant velocity across the sheet, which varied only because of the area reduction as the crack moved. Propellant data were obtained at 0 and 500 psig inside a pressure chamber over a temperature range of 40°–120°F and shifted for viscoelastic effects (Fig. 10).

The enhancement of resistance to propagation is evident, since considerably higher stress intensity factors are required to propagate a crack at a given velocity under pressure as compared to the same situation without pressure.

Rocket motors operating under chamber pressure have a built-in safety factor from the pressure. Plane stress cross-sectional slices were fabricated from propellant and tested in the same manner as the Solithane specimens.

K_I was determined for a variety of circular port designs with the PBAN propellant. Thicker web designs were selected for test and analysis because of the higher modulus and toughness of the solid propellant. Curves for stress intensity factor vs crack length are presented in Fig. 11.

The propellant grain slice tests included four web thicknesses. Zero stress temperatures varied between 146° and 150°F for the PBAN propellant.

Solid propellant circular port grains were tested remotely using a high-speed pressurization system. Typical pressure rise times were 110 msec. Crack displacement data were obtained by high-speed motion pictures using backlighting to emphasize the crack tip. Tests were conducted at 60°, 92°, and 126°F under the conditions presented in Table 1. None of the propellant geometries exhibited crack growth. The cracks opened similarly to the Solithane samples, but remained stationary for the duration of the pressure period.

Table 1 Propellant grain test data

Test	Test temperature, °F	Peak pressure, psi	Rise time, msec	b/a ratio	Initial crack length from bore surface, in.	Zero stress temperature, °F
1	60	270	60	9.3	0.50	148
2	60	545	120	8.0	0.50	149
3	60	730	120	7.0	0.50	150
4	60	625	110	13.5	0.50	146
5	92	740	110	6.8	0.50	150
6	92	630	110	8.0	0.50	149
7	126	690	110	7.0	0.50	150

Calculations for the propellant grain slices using the pressure-enhanced crack velocity data (Fig. 10) predicted that the cracks would not propagate at pressure levels less than 750 psig. This pressure level could not be achieved because the Plexiglas case material ruptured at pressures lower than 750 psi. If the pressure-enhanced fracture characteristics had been neglected, slow crack propagations at 560 psi would have been predicted.

Pressure enhanced properties were also demonstrated on uniaxial tensile tests run on the propellant (Fig. 12), but not on the Solithane 113. Pressure enhancement of the propellant differed for the biaxial fracture and the uniaxial tensile test results. At 500 psi, the fracture enhancement factor was 1.35, while the comparable uniaxial stress enhancement was 1.58. This pressure-sensitive material behavior is common for highly filled polymeric materials where the particles separate from the rubber at very low strain levels.

Comparison of Theory and Experiment

The total K_I for the pressurized grain consists of the pressurization component plus the thermal load from the zero stress temperature to the pressurization test temperature. Linear superposition led to the equation

$$K_{I(\text{total}} = K_{I(\text{thermal})} + K_{I(\text{pressure})} \tag{22}$$

Numerical analysis was conducted to define the thermal and pressurization K_I components. The total K_I evaluated from Eq. (22) was used to predict Solithane 113 crack length histories (Fig. 6). These theoretical K_I predictions are compared to the experimental results shown in Fig. 13. Initial erratic crack growth behavior near the razor cut was neglected. The experimental K_I was determined from actual crack displacement data and from the mean value of the master K_I vs $\dot{c}a_T$ curve for Solithane 113. Comparison of mean values of the experimental and theoretical K_I's shows a maximum deviation at the 0.5-in. crack length. However, this is the region of the man-made flaw. For crack lengths of 0.8–2 in., the variation from the theoretical mean ranges from 0% to 20%. The theoretical K_I curve has a band which

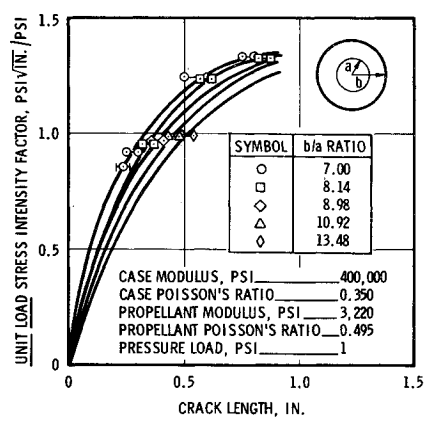

Fig. 11 Computed pressure K_I vs crack length for PBAN propellant.

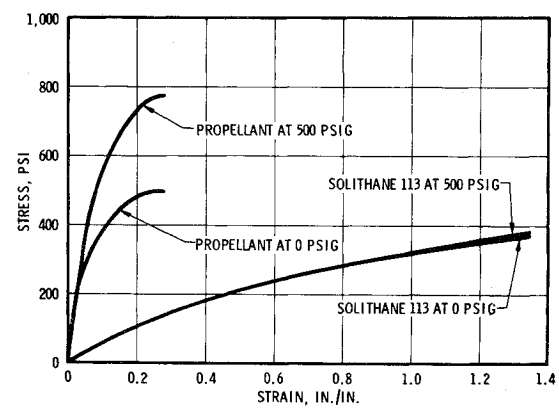

Fig. 12 Pressure enhancement for propellant and Solithane 113.

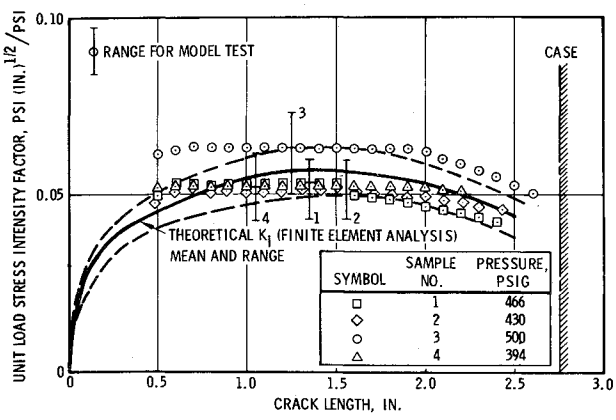

Fig. 13 Comparison of K_I values for Solithane 113 two-dimensional pressurization tests, $b/a = 4.5$.

represents modulus, Poisson's ratio, and finite element calculation errors. Predicted K_I values have a range of $\pm 9\%$, which is attributed to a Poisson's ratio sensitivity where ν varies between 0.4999 and 0.490. Nearly incompressible materials always exhibit this sensitivity when used in structural applications.

The maximum range of experimental K_I ($\pm 17\%$) determined using Fig. 3 is shown as a band for each test in Fig. 13. The mean deviation from the predicted K_I at 1.4-in. crack length is 6.1%, 9.4%, 10.5%, and 8.8% for samples 1, 2, 3, and 4, respectively. This deviation is a function of the crack length, and the mean theoretical K_I never falls outside the maximum range of the experimental K_I's once the crack length has progressed 0.25 in. beyond the manufactured flaw.

The large data scatter is generated by the uncertainty in the conversion from model crack velocity to K_I, which is accomplished using Fig. 3. This type of data scatter is typical for failure and fracture response of filled and unfilled polymeric materials.

The K_I method was selected for comparing theory with experiment because very small changes in K_I or a_T values cause large variations in crack velocities. Since fracture analysis is very sensitive to small variations in material properties, they must be obtained using extremely accurate testing techniques. An error of even a few degrees in the zero stress temperature has a significant effect on crack velocity predictions.

Conclusions

The viscoelastic fracture mechanics predictions of crack velocity or K_I (Fig. 13) for the two-dimensional geometries are in agreement with the laboratory determined fracture toughness behavior of Solithane 113 (Fig. 3). This correspondence is limited by experimental error and material property sensitivity, which enters into the theoretical calculations, as well as by the evaluation of K_I from the model tests. Crack propagation could not be induced with solid propellant grain models, because of an increase in fracture toughness in a hydrostatic stress field. Fracture properties with hydrostatic pressure are improved using highly filled polymers which exhibit internal bond failure between the filler and binder material.

Initial crack growth from induced cracks was erratic compared to that observed after the natural crack tip geometry developed in the test material. This behavior was expected for fracture tests and justifies inducing natural cracks in fracture specimens. Crack velocities are slow and controllable in viscoelastic material, so the initial growth from fabricated cracks can be disregarded while later reliable crack growth data can be used for fracture characterization. The analytic predictions of crack growth histories were very sensitive to small variations in temperature and some material properties. This sensitivity follows from the shift factor relationship for the temperature effect. Despite this temperature and material property sensitivity, the confirmation of theory was excellent.

The solid propellant exhibited a unique pressure sensitivity which is not experienced by conventional structural materials. This pressure sensitivity improved the fracture properties and stopped fracture propagation in grain slice tests. This enhancement in fracture behavior reduces the possibility of crack propagation during ignition of a solid propellant motor.

References

[1] Griffith, A. A., "The Phenomena of Rupture and Flow in Solids," *Philosophical Transactions of the Royal Society*, Vol. 221, 1920, pp. 163–198.

[2] Williams, M. L., "Initiation and Growth of Viscoelastic Fracture," *International Journal of Fracture Mechanics*, Vol. 1, No. 4, 1965, pp. 294–310.

[3] Williams, M. L., "The Relation of Continuum Mechanics to Adhesive Fracture," *Journal of Adhesion*, Vol. 4, 1972, pp. 307–332.

[4] Swanson, S. R., "Crack Propagation in Solid Rocket Propellant Grains Under Ignition Loading," M.S. thesis, June 1968, Dept. of Mechanical Engineering, University of Utah, Salt Lake City, Utah.

[5] Chan, S. K., Tuba, I. S., and Wilson, W. K., "On the Finite Element Method in Linear Fracture Mechanics," Scientific Paper 68-107-FMPWR-P1, April 1968, Westinghouse Research Labs., Pittsburgh, Pa.

[6] Kobayashi, A. S., Maiden, D. E., Simon, B. J., and Iida, S., "Application of Finite Element Analysis to Two-Dimensional Problems in Fracture Mechanics," Paper 69-WA/PVP-12, 1969, ASME, New York.

[7] Deverall, L. I. and Lindsey, G. H., "A Comparison of Numerical Methods for Determining Stress Intensity Factors," *Transactions of the ASME, Journal of Basic Engineering*, Vol. 94, June 1972, pp. 508–509.

[8] Mueller, H. K., "Stress-Intensity Factor and Crack Opening for a Linearly Viscoelastic Strip with a Slowly Propagating Central Crack," *International Journal of Fracture Mechanics*, Vol. 7, No. 2, 1971, pp. 129–141.

[9] Mueller, H. K. and Knauss, W. G., "Crack Propagation in a Linearly Viscoelastic Strip," *Journal of Applied Mechanics*, Vol. 38, No. 2, June 1971, p. 483.

[10] Knauss, W. G., "Delayed Failure—The Griffith Problem for Linearly Viscoelastic Materials," *International Journal of Fracture Mechanics*, Vol. 6, No. 1, 1970, pp. 7–20.

[11] Williams, M. L., Landel, R. F., and Ferry, J. D., "The Temperature Dependence of Relaxation Mechanism in Amorphous Polymers and Other Glass-Forming Liquids," *Journal of American Chemical Society*, Vol. 77, 1955, pp. 3701–3707.

[12] Irwin, G. R., "Fracture," *Encyclopedia of Physics*, Vol. VI, Springer-Verlag, Berlin, 1958, pp. 551–590.

[13] Becker, E. B. and Brisbane, J. J., "Application of the Finite Element to Stress Analysis of Solid Propellant Rocket Grains," Rept. S76, 1966, Rohm and Haas Co., Redstone Research Div., Huntsville, Ala.

[14] Francis, E. C., Lindsey, G. H., and Parmerter, R. R., "Pressurized Crack Behavior in Two-Dimensional Rocket Motor Geometries," *Journal of Spacecraft and Rockets*, Vol. 9, No. 6, June 1972, pp. 415–419.